Protein-modified ultra-small gold clusters for dual-modal *in vivo* fluorescence/photoacoustic imaging

Duyang Gao, Yubin Liu, Yating Wang, Zhen Yuan

Faculty of Health Sciences, University of Macau, Taipa, Macau SAR, China

Correspondence to: Zhen Yuan. Faculty of Health Sciences, University of Macau, Taipa, Macau SAR, China. Email: zhenyuan@umac.mo.

Background: Construction of nanoprobes for dual-modal fluorescence/photoacoustic imaging (PAI) is of great importance for the detection of disease pathology and the development of innovative therapeutics. Previously ultra-small gold clusters were designed and used as contrast agents for fluorescence imaging (FLI). However, it is not clear whether they can also serve as promising probes for PAI. In this study, protein-modified ultra-small gold clusters are produced and examined quantitatively as enhanced contrast agents for dual-modal *in vivo* fluorescence and PAI.

Methods: To construct the dual-modal ultra-small gold clusters, $HAuCl_4 \cdot 4H_2O$ aqueous solution was first mixed with the protein solution. NaOH was further introduced to the solution under vigorous stirring. The as-designed dual-modal nanoprobe was formed after stirring for 2 h at 65 ℃. And then the solution was purified by gel column for further application. Zebrafish, cultivated in the solution containing gold clusters, was used in this study to demonstrate the dual-modal imaging ability of the nanoprobe by using our home-made optical-resolution photoacoustic microscopy and commercial fluorescence microscopy systems.

Results: The gold nanoclusters were synthesized with diameters of about 3 nm, which showed the broad absorption with a characteristic peak centered at 520 nm. A strong near-infrared emission ranging from 600 to 750 nm was also observed for the gold clusters. In addition, the cell viability was more than 90% even at a high concentration of the nanoprobes. The zebrafish cultivated with the gold clusters exhibited dramatically enhanced fluorescence and photoacoustic signal intensities.

Conclusions: Quantitative analysis results demonstrated that BSA-modified gold clusters were excellent contrast agents for *in vivo* dual-modal fluorescence/PAI. Due to their ultra-small size and superior biocompatibility, they can be applied to the detection and treatment of various diseases with enhanced sensitivity.

Keywords: Gold clusters; dual-modal nanoprobe; *in vivo* zebrafish imaging; optical-resolution photoacoustic imaging system

Introduction

Recent trends in biomedical imaging reflect the shift from producing high-resolution anatomical images to generating direct functional information of biological tissues. Although the present structural imaging modalities including X-ray, MRI, ultrasound and CT are well-examined for various clinical applications, it is very challenging for these modalities to image biological tissues at the cellular, vascular or biochemical levels, which may be better suited for disease diagnosis and prognosis (1,2). Consequently, it is essential to develop non-invasive and functional imaging technologies that can detect early-stage diseases, guide disease treatment and even perform the therapy.

Among different functional biomedical imaging methods that can resolve the basic limitations of X-ray, CT, ultrasound

or MRI, laser-induced photoacoustic imaging (PAI) are very promising (3,4). To date, PAI is rapidly growing, largely because PAI can reconstruct both the functional and structural information of biological tissues with high optical contrast, high ultrasound resolution and satisfactory penetration depth (5-11). However, the endogenous contrast of PAI may be insufficient for disease detection in case that the interaction of light with tissue is not disease-specific. Therefore, there is a role for exogenously administered contrast enhancing agents that have an affinity for the disease site through biochemical interactions, providing not only sensitive but also disease-specific signals. Meanwhile, among all the molecular imaging modalities, fluorescence imaging (FLI) has been widely used in biomedical field due to its high sensitivity (12). In particular, as an *in vivo* functional imaging modality, FLI plays an essential role in the study of cellular level events such as gene and protein expressions, cancer early detection and treatment (13,14). To take advantages of the complementary information from these two optical imaging modalities, we present an optimized approach that combines FMI and PAI to improve the *in vivo* imaging sensitivity. More importantly, we determine to develop a novel optical imaging approach that combines multifunctional nanoprobes with advanced optical imaging instrumentation for accurately *in vivo* imaging. We believe the developed imaging system with the utilized nanoprobes will be able to recover images of biological tissues with high accuracy and molecular specificity.

In this study, ultra-small gold clusters will be designed as dual-modal multifunctional nanoprobes for FLI/PAI. Interestingly, according to the source of the function, the nanoprobes can be mainly divided into two types. One category is "all in one", which means integrating different functional components into one particle. Another type is "one for all" that can exhibit multifunctional properties by one element. "All in one" type multifunctional nanoprobes always refers to complicated steps, which makes it hard to reproduce (15). Therefore, constructing and opening a new application field of "one for all" type multifunctional nanoprobes is of great significance. For the present work, ultra-small gold clusters will be designed as dual-modal nanoprobes for FLI and PAI. To produce the dual-modal ultra-small gold clusters, $HAuCl_4 \cdot 4H_2O$ aqueous solution will be first mixed with the protein solution. NaOH is then put into the solution under vigorous stirring. The as-designed dual-modal nanoprobe is synthesized after stirring for 2 h at 65 ℃. In particular, the developed nanoprobe has its unbeatable advantages for the detection of diseases

due to its ultra-small size and excellent biocompatibility. In addition, adult zebrafish (16,17) were chosen as the animal model due to their small size, which were more suitable for photoacoustic and fluorescence microscopy imaging. Specifically, they have also been produced to model various human diseases including congenital heart disease, Alzheimer's disease, malignant melanoma, and so on. In this study, zebrafish, cultivated in the solution containing gold clusters, will be used to demonstrate the dual-modal imaging ability of the nanoprobe by using the home-made optical-resolution PAI system and commercial FLI setup.

Methods

Materials, characterization and synthesis of BSA-modified gold clusters

Sodium hydroxide (NaOH, 99.99%), bovine serum albumin (66 kDa), polyethylene glycol (PEG, MW 3350), $HAuCl_4 \cdot 4H_2O$, nitric acid (HNO$_3$, 65%), Sephacryl S-300 HR, hydrochloric acid (HCl, 37%), Triton-X 100, and ethanol were obtained from Sigma-Aldrich. Fetal bovine serum (FBS), phosphate-buffered saline (PBS, pH 7.4), and Dulbecco's Modified Eagle's Medium (DMEM) were purchased from Gibco Life Technologies. Double-distilled water (18.25 M$\Omega \cdot$cm, 25 ℃) was used to prepare all solutions.

Gold clusters with ultra-small size were prepared according to the previous report (18). In a typical experiment, the glassware was first washed with aqua regia, and then rinsed with ethanol and ultrapure water, respectively. $HAuCl_4 \cdot 4H_2O$ aqueous solution was added to BSA solution with a concentration of 50 mg$\cdot$mL^{-1} under vigorous stirring. NaOH solution was then introduced to adjust the pH value of the solution. The color of the solution changed from light yellow to light brown, and then to deep brown under vigorous stirring at 65 ℃. The reaction was finally completed in 2 h.

A series of stock solutions were prepared including BSA [2% (w/v), 10 mL], PEG [5% (w/v), 100 mL] and Triton-X 100 [0.25% (w/v), 100 mL]. The eluent was then prepared by mixing double-distilled water (96 mL), HEPES buffer (1 M, 2 mL), and polyethylene glycol (5%, 2 mL). Sephacryl S-300 HR gel column was washed at least three times using the eluent. 1 mL of the as-prepared gold clusters which was required to be purified, was mixed with HEPES buffer (1 M, 20 μL), PEG (5%, 20 μL), Triton-X 100 (0.25%, 20 μL), and BSA (2%, 20 μL). The mixture was then left on the
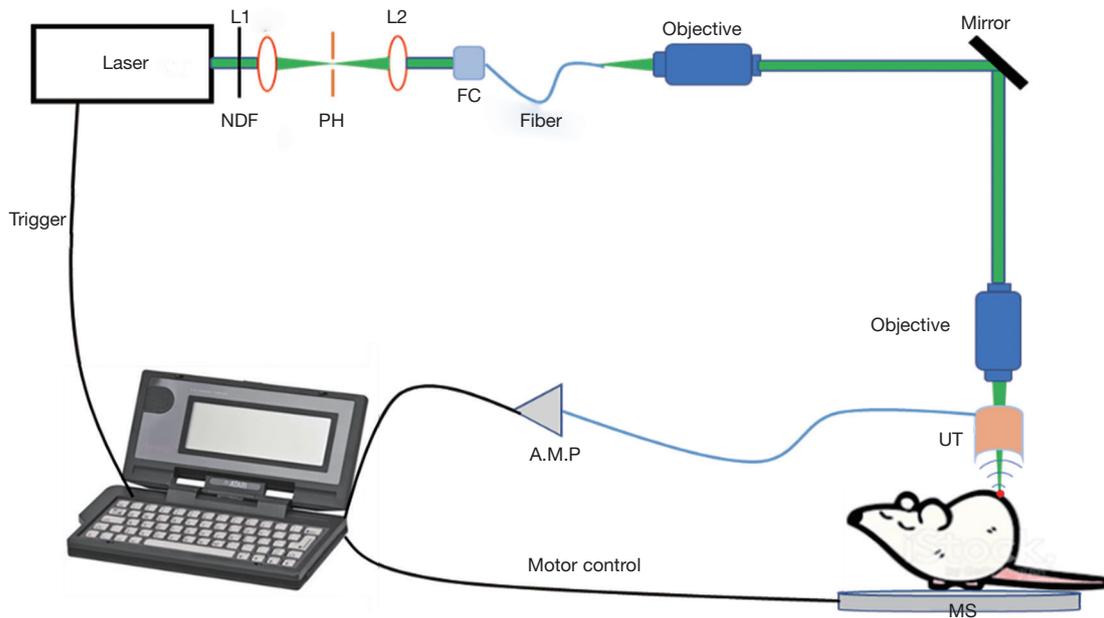
Figure 1 The home-made optical-resolution PA microscopy system. NDF, neutral density filter; MS, motor stage; PH, pinhole; AMP, amplifier; FC, Fiber coupler; UT, ultrasonic transducer.

rotary shaker for 1 h. Finally, the resulting BSA-modified gold clusters were separated from free BSA and alkaline solvent by gel filtration using Sephacryl HR-300 gel media.

The optical-resolution photoacoustic microscopy and fluorescence microscopy systems

Figure 1 showed our home-made optical-resolution photoacoustic (PA) microscopy system. In this system, 532 nm laser with a pulse width of 1 ns and a repetition rate up to 5 KHz was used as the excitation light source for PA imaging. The laser beam first passed through an optical subsystem (NDF: neutral density filter; L1 & L2: focusing lens; PH: pinhole; FC: optical fiber coupler), and then coupled into a single-mode fiber. Then the laser beam delivered by the fiber passed through an objective and changed the direction of transmission by a mirror. To generate a high-resolution PA image, an objective was adopted to focus the laser beam on the sample. A motor stage was used for scanning the sample. The ultrasonic transducer was specially designed with a pinhole in the center so that the focused laser facula can pass through this pinhole on the transducer. The PA signal detected by the ultrasonic transducer was amplified by the amplifier and collected on the computer for optical-resolution PA microscopy imaging.

By contrast, the fluorescence microscopy system used is a commercial imaging setup (Nikon eclipse Ni-U), which includes three parts: CCD, achromatic condenser, and mercury lamp (*Figure 2*). During the FLI procedure, CCD is placed upon the top of the fluorescence microscope and the achromatic condenser will be set up on the base stage. After adjusting the focus of the objective on the sample with mercury on, CCD camera can generate the image.

In vivo imaging

Male wild adult zebrafish (*Figure 3*) were used for the present work. Zebrafish were maintained in our flow-through aquaria at temperature 28±0.5 ℃ with the photoperiod of 14 h of light and 10 h of dark. All procedures were performed in compliance with the guidelines on animal research stipulated by the Animal Care and Use Committee with the University of Macau. Zebrafish were then cultivated in the gold clusters solution for 2 h before *in vivo* dual-modal imaging.

Results

The as-obtained BSA-Au clusters were first characterized by transmission electron microscopy (TEM) image. *Figure 4A* showed that the as-prepared BSA-Au clusters were dispersed

Figure 2 The fluorescence microscopy system.

Figure 3 Photograph of the representative zebrafish.

well with an overall diameter of about 3 nm in the PBS buffer solution. The UV-Vis absorption and fluorescent emission spectra of the BSA-modified gold clusters in PBS were provided in *Figure 4B*. The surface plasma resonance absorption peak of the developed nanoprobes was centered at about 520 nm. The hydrodynamic diameter and zeta potential of the as-obtained BSA-modified gold clusters dispersed in PBS were also quantified using dynamic light scattering (DLS) analysis. It demonstrated that the effective hydrophilic size was about 11.5 nm, which was much larger than that of TEM (*Figure 4C*). It can be ascribed to the BSA layer, which is hard to detect by TEM. In addition, a thin electric dipole layer of the solvents adhered to the gold clusters can also be determined by DLS. Furthermore, the generated results also indicated that the as-synthesized gold clusters dispersed well, in accordance with the TEM image (*Figure 4A*). The Zeta potential of the gold clusters was about 21 mV below zero (*Figure 4D*), which was a proper charge to stabilize the clusters in the biological environment.

Before the *in vivo* FLI/PAI, the cytotoxicity of the BSA-modified gold clusters was measured with the usage of standard CCK-8 assay. As shown in *Figure 5*, the cell viability was more than 90% even at the high concentration of 1.5 mg·mL^{-1}. The results indicated that the nanoprobes exhibited no significant cytotoxicity after 12 and 24 h incubation with the 293T cells (*Figure 5A*) and 4T1 cells (*Figure 5B*).

To demonstrate the *in vivo* dual-modal imaging ability of as-obtained gold clusters, we performed *in vivo* FLI/PAI of zebrafish by using our home-made optical-resolution PA imaging system. As shown in *Figure 6* (top image), enhanced fluorescence signal can be clearly observed in the organs as indicated by the white circle. Meanwhile, increased PA signals were also detected upon the similar organs (bottom image of *Figure 6*). The quantitative analysis results were displayed on the right of *Figure 6*. Our imaging results demonstrated that the intensity of FL signal increased about seven times after cultivation with the contrast agents, whereas the PA signals were enhanced more than twice.

Discussion

Zebrafish is a powerful animal model to study human diseases and develop high-throughput screens for effective treatment (19). However, it is hard to identify and confirm the differences between the normal and disease tissues especially at their adult stage by using one imaging modality. Consequently, the development of new imaging techniques and contrast agents that combines more than one molecular imaging modalities are able to provide high-sensitivity detection of various diseases. In this study, home-made optical-resolution PA systems combined with commercial fluorescence microscopy systems were used for adult zebrafish imaging (20). The system and the adult zebrafish model were further used to evaluate the dual-modal imaging ability of the as-prepared gold clusters.

It was noted that the absorption peak of the gold clusters was nearly at wavelength 532 nm, which was precisely adequate for PAI. In addition, the fluorescence emission of the nanoprobe was at the near-infrared region (650–900 nm), which was a benefit to *in vivo* FLI due to its deep penetration in tissues. Interestingly, although the gold nanoclusters were used as contrast agents for *in vivo* FLI, they were not inspected for PAI previously. Our study demonstrated for the first time that protein-modified ultra-small gold clusters can also serve as contrast
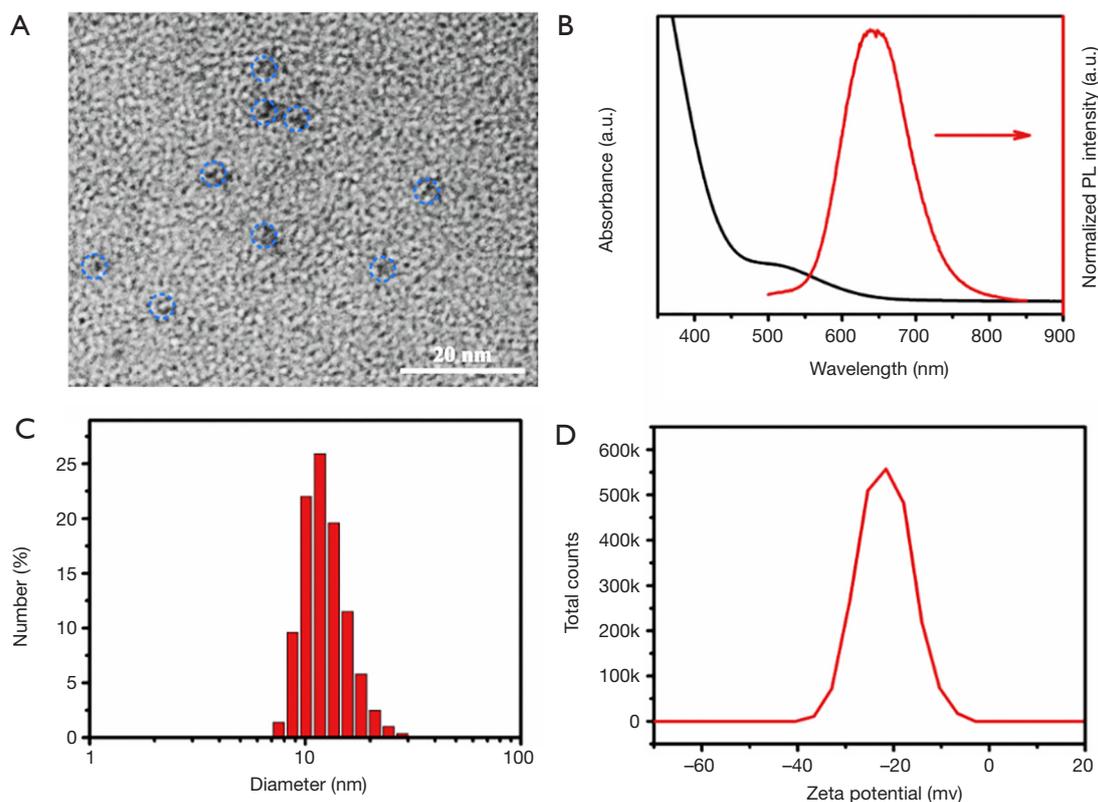
Figure 4 Characterization of BSA-Au clusters. (A) TEM image, (B) UV-Vis absorption and fluorescence emission spectra, (C) hydrodynamic diameter, and (D) zeta potential of the as-prepared BSA-modified gold clusters. Blue circles indicate the gold clusters.
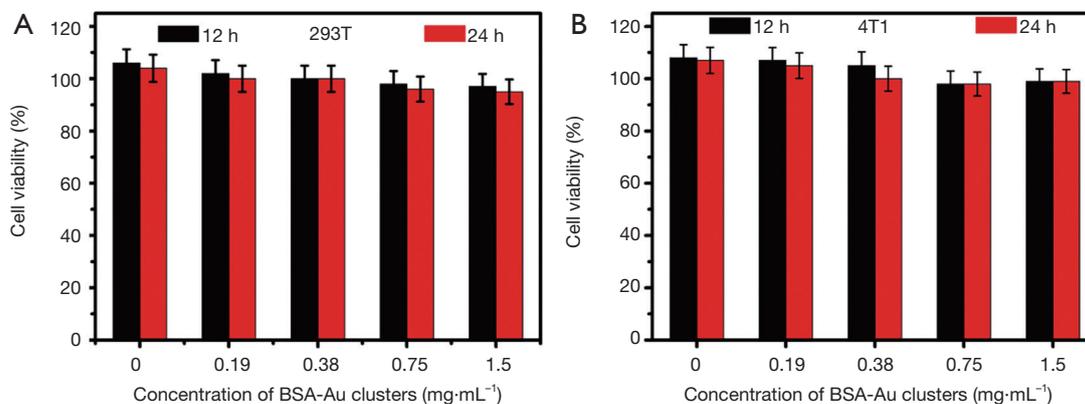

Figure 5 Cell viability of 293T cells (A) and 4T1 cells (B) recorded after being incubated with BSA-modified gold clusters at various concentrations (0, 0.19, 0.38, 0.75, 1.5 mg·mL^{-1}).

agents for *in vivo* PAI. FLI was widely applied for tissue imaging due to their high sensitivity, whereas PAI exhibited the advantages in penetration depth for *in vivo* imaging (21,22). The combination of the two imaging modalities made it possible to capture more functional information

of biological tissues. Compared with other contrast agents for FLI/PAI, the gold clusters can realize the dual-modal imaging without conjugating other functional blocks. Therefore, it was simple to obtain the nanoprobes in one step, which made it easy to reproduce. Moreover, protein-
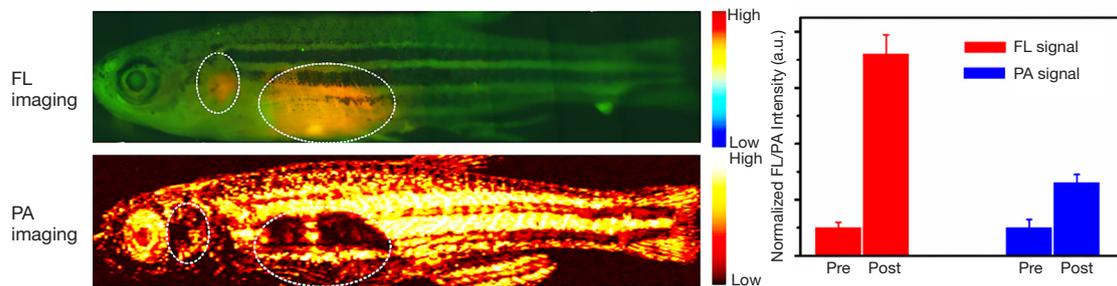
Figure 6 *In vivo* FLI/PAI of zebrafish. *In vivo* FLI (top image), *in vivo* PAI of zebrafish (bottom image), and quantitative analysis of the fluorescence and PA signals (right). Noted that the white circles indicate the fluorescence or PA signals of the BSA-modified gold clusters. FLI, fluorescence imaging; PAI, photoacoustic imaging.

modified ultra-small gold clusters were composed of protein and environment-friendly elements, which made it had excellent biocompatibility and suitable for *in vivo* imaging. Moreover, the protein used to protect the gold clusters can also be linked with drugs for treatment due to their abundant reactive groups including carboxyl groups and amine groups. According to the anatomy of the zebrafish published previously (23), our findings demonstrated that the organs with enhanced fluorescence/PA signals included the swim bladder, spleen, gills, intestinal bulb, pancreas, and posterior intestine. Our study also validates that the as-prepared gold clusters can serve as contrast agents for fluorescence/PA dual-modal imaging.

Conclusions

In summary, we have constructed ultra-small gold clusters with excellent biocompatibility and near-infrared emission in the presence of protein. The as-prepared protein-modified nanoprobes can serve as contrast agents for both FLI and PAI. By leveraging the home-made optical-resolution PA microscopy and commercial fluorescence microscopy systems, the nanoprobes proved to be good contrast agents for *in vivo* dual-modal zebrafish imaging. More importantly, our *in vivo* imaging results also demonstrated that the nanoprobes can be applied to the detection and treatment of different diseases with an enhanced sensitivity and accuracy.

Acknowledgements

Footnote

Conflicts of Interest: The authors have no conflicts of interest to declare.

References

1. Yuan Z, Zhang Q, Sobel ES, Jiang H. Tomographic x-ray-guided three-dimensional diffuse optical tomography of osteoarthritis in the finger joints. J Biomed Opt 2008;13:044006.
2. Bonadonna G, Valagussa P, Brambilla C, Ferrari L, Moliterni A, Terenziani M, Zambetti M. Primary chemotherapy in operable breast cancer: eight-year experience at the Milan Cancer Institute. J Clin Oncol 1998;16:93-100.
3. Wang LV, Hu S. Photoacoustic tomography: in vivo imaging from organelles to organs. Science 2012;335:1458-62.
4. Hong G, Lee JC, Robinson JT, Raaz U, Xie L, Huang NF, Cooke JP, Dai H. Multifunctional in vivo vascular imaging using near-infrared II fluorescence. Nat Med 2012;18:1841-6.
5. Zhang EZ, Laufer JG, Pedley RB, Beard PC. In vivo high-resolution 3D photoacoustic imaging of superficial vascular anatomy. Phys Med Biol 2009;54:1035-46.
6. Agarwal A, Huang S, O'donnell M, Day KC, Day M, Kotow N, Ashkenazi S. Targeted gold nanorod contrast agent for prostate cancer detection by photoacoustic imaging. J Appl Phys 2007;102:064701.
7. Yuan Z, Li X, Xi L. Listening to light scattering in

turbid media: quantitative optical scattering imaging using photoacoustic measurements with one-wavelength illumination. J Opt 2014;16:06530.

8. Liu Y, Jiang H, Yuan Z. Two-scheme for quantitative photoacoustic tomography based on Monte Carlo simulation. Med Phys 2016;43:3987.

9. Liu Y, Yuan Z. Multi-spectral photoacoustic elasticity tomography. Biomed Opt Express 2016;7:3323-34.

10. Gao D, Sheng Z, Liu Y, Hu D, Zhang J, Zhang X, Zheng H, Yuan Z. Protein-Modified CuS Nanotriangles: A Potential Multimodal Nanoplatform for In Vivo Tumor Photoacoustic/Magnetic Resonance Dual-Modal Imaging. Adv Healthc Mater 2017;6:1601094.

11. Zhang J, Chen HB, Zhou T, Wang LM, Gao DY, Zhang XJ, Liu YB, Wu CF, Yuan Z. A PIID-DTBT based semiconducting polymer dot with broad and strong optical absorption in the visible-light region as a highly-effective contrast agent for multiscale and multi-spectral photoacoustic imaging. Nano Research 2016;10:64-76.

12. Ntziachristos V, Ripoll J, Wang LV, Weissleder R. Looking and listening to light: the evolution of whole-body photonic imaging. Nat Biotechnol 2005:23:313-20.

13. Luker GD, Luker KE. Optical imaging: Current applications and future directions. J Nucl Med 2008;49:1-4.

14. Ntziachristos V, Tung CH, Bremer C, Weissleder R. Fluorescence molecular tomography resolves protease activity in vivo. Nat Med 2002;8:757-61.

15. Gao D, Yuan Z. Photoacoustic-Based Multimodal Nanoprobes: from Constructing to Biological Applications.

16. Liu Y, Li DL, Yuan Z. Photoacoustic tomography imaging of the adult zebrafish by using unfocused and focused high-frequency ultrasound transducer. Applied Sciences 2016;6:392-4.

17. Zhang J, Pun SH, Yu Y, Gao D, Wang J, Mak PU, Lei KF, Cheng CH, Yuan Z. Development of a multi-band photoacoustic tomography imaging system based on a capacitive micromachined ultrasonic transducer array. Appl Opt 2017;56:4012-8.

18. Xie J, Zheng Y, Ying JY. Protein-directed synthesis of highly fluorescent gold nanoclusters. J Am Chem Soc 2009;131:888-9.

19. Langenau DM, Traver D, Ferrando AA, Kutok JL, Aster JC, Kanki JP, Lin S, Prochownik E, Trede NS, Zon LI, Look AT. Myc-induced T cell leukemia in transgenic zebrafish. Science 2003;299:887-90.

20. Wang LV. Multiscale photoacoustic microscopy and computed tomography. Nat Photonics 2009;3:503-9.

21. Gao DY, Zhang PF, Sheng ZH, Hu DH, Gong P, Chen C, Wan Q, Gao GH, Cai LT. Highly bright and compact alloyed quantum rods with near infrared emitting: a potential multifunctional nanoplatform for multimodal imaging in vivo. Adv Funct Mater 2014;24:3897-905.

22. Nie L, Chen X. Structural and functional photoacoustic molecular tomography aided by emerging contrast agents. Chem Soc Rev 2014;43:7132-70.

23. White R, Rose K, Zon L. Zebrafish cancer: The state of the art and the path forward. Nat Rev Cancer 2013;13:624-36.

Int J Biol Sci 2017;13:401-12.